Published in IET Image Processing
Received on 6th March 2013
Revised on 20th October 2013
Accepted on 2nd November 2013
doi: 10.1049/iet-ipr.2013.0178

ISSN 1751-9659

Effective fuzzy clustering algorithm with Bayesian model and mean template for image segmentation

Hui Zhang[1,2,3], Qing Ming Jonathan Wu[2], Yuhui Zheng[1,3], Thanh Minh Nguyen[2], Dingcheng Wang[1,3]

[1]*School of Computer & Software, Nanjing University of Information Science & Technology, Nanjing, People's Republic of China*
[2]*Department of Electrical and Computer Engineering, University of Windsor, Windsor, ON, Canada*
[3]*Jiangsu Engineering Center of Network Monitoring, Nanjing University of Information Science & Technology, Nanjing, People's Republic of China*
E-mail: jwu@uwindsor.ca

Abstract: Fuzzy c-means (FCMs) with spatial constraints have been considered as an effective algorithm for image segmentation. The well-known Gaussian mixture model (GMM) has also been regarded as a useful tool in several image segmentation applications. In this study, the authors propose a new algorithm to incorporate the merits of these two approaches and reveal some intrinsic relationships between them. In the authors model, the new objective function pays more attention on spatial constraints and adopts Gaussian distribution as the distance function. Thus, their model can degrade to the standard GMM as a special case. Our algorithm is fully free of the empirically pre-defined parameters that are used in traditional FCM methods to balance between robustness to noise and effectiveness of preserving the image sharpness and details. Furthermore, in their algorithm, the prior probability of an image pixel is influenced by the fuzzy memberships of pixels in its immediate neighbourhood to incorporate the local spatial information and intensity information. Finally, they utilise the mean template instead of the traditional hidden Markov random field (HMRF) model for estimation of prior probability. The mean template is considered as a spatial constraint for collecting more image spatial information. Compared with HMRF, their method is simple, easy and fast to implement. The performance of their proposed algorithm, compared with state-of-the-art technologies including extensions of possibilistic fuzzy c-means (PFCM), GMM, FCM, HMRF and their hybrid models, demonstrates its improved robustness and effectiveness.

1 Introduction

Image segmentation is one of the most important and difficult problems in many real-world applications, such as robot vision, object recognition and medical image processing. Although different methodologies [1–4] have been proposed for image segmentation, it remains a challenge because of overlapping intensities, low contrast of images and noise perturbation. In the past decades, fuzzy segmentation methodologies, and especially the fuzzy c-means (FCMs) algorithms [5], have been widely studied and successfully applied in image clustering and segmentation. Their fuzzy nature makes the clustering procedure able to retain more original image information than the crisp or hard clustering methodologies [6, 7].

Although the standard FCM algorithm usually performs well with non-noise images, it is still weak in the presence of noise, outliers and other imaging artefacts. This may be caused by two aspects: one is the usage of the non-robust, Euclidean distance function, and the other does not pertain to any information about spatial context. Several attempts have been made to compensate for these drawbacks of FCM. For example, in [8–11], various more robust alternatives for the distance function of the FCM algorithm have been proposed. In [12], Tran and Wagner introduced the fuzzy mixture weights by redefining FCM distance function for speaker recognition. In [13], Ramathilaga *et al.* combined mean variable distance and centre learning method for image clustering. In [14, 15], various FCM-type clustering schemes, incorporating spatial constraints into the fuzzy objective function, have been proposed. In [16], Chuang *et al.* introduced the spatially weighted FCM (SWFCM) which incorporates spatial information into the membership function for clustering. However, all the methods mentioned above still have significant disadvantages such as limited robustness to outliers and high-computational complexity. Inspired by Gaussian mixture model (GMM), in this paper, we deal with the traditional FCM in a Bayesian way to overcome the limitations mentioned above.

One of the most widely used clustering models for image segmentation is the well-known finite mixture model (FMM) [1]. The GMM is most commonly selected as a particular case of the FMM by assuming the conditional probability as a Gaussian distribution [17–19]. The GMM is a flexible and powerful statistical modelling tool for multivariate data classification. The main advantage of the standard GMM is that it is easy

to implement and the small number of parameters in GMM can be efficiently estimated by adopting the expectation maximisation (EM) algorithm. However, as a histogram-based model, the GMM assumes that each pixel in an image is independent of its neighbours, and does not take into account spatial dependencies. Furthermore, it does not use the prior knowledge that adjacent pixels most likely belong to the same cluster. Thus, the performance of the GMM is sensitive to noise and image contrast levels.

To overcome this limitation, a wide variety of approaches have been proposed to incorporate the spatial information into the image. A common approach is the use of the hidden Markov random field (HMRF) model [20, 21]. In the HMRF model, the spatial information in an image is encoded through the contextual constraints of neighbouring pixels, which are characterised by conditional HMRF distributions. Parameter estimation in HMRF models usually rely on maximum likelihood (ML) or Bayesian methods. Besag [22] introduces the idea of the pseudo likelihood approximation when ML estimation is intractable.

In this paper, we combine the benefits of FCM and GMM to propose a new algorithm for image segmentation. To combine the merit of FCM and GMM models, we first introduce the Kullback–Leibler (KL) divergence information to regularise the fuzzy objective function with the consideration of prior probability and posterior probability (fuzzy membership), simultaneously. Secondly, we consider the labelling of a pixel to be influenced by the labels in its immediate neighbourhood to incorporate more spatial information into the image. Moreover, we add weighting for distant pixels in order to distinguish among the contributions of different pixels, as the weighted parameters decrease with the increasing distance from the central pixel. Thirdly, in our model, the distance function is measured by multivariate Gaussian function instead of the traditional Euclidean distance (L_2 norm) in the standard FCM algorithm. Thus, GMM can be considered as a special case of our model. Finally, we select mean template instead of HMRF as the spatial constraint for image segmentation. The main drawback of HMRF model is that it is computationally expensive to implement, and require the additional parameter β to control the degree of image smoothness. The chosen parameter β has to be both large enough to tolerate the noise, and small enough to preserve image sharpness and details. Thus, the parameter is noise dependent to some degree and selected generally based on experience. In our algorithm, the prior probability of an image pixel is influenced by the fuzzy membership (or posterior probability) of pixels in its immediate neighbourhood with the help of a mean template. Different from the HMRF model, our model is fully free of the empirically adjusted parameter β. The proposed algorithm is applied to segment synthetic images, real images and red green blue (RGB) colour images. The performance of our proposed approach, compared with state-of-the-art technologies, demonstrates its improved robustness and effectiveness.

The remainder of this paper is organised as follows: in Section 2, we provide a brief review of the FCM algorithm. In Section 3, we introduce our algorithm based on the FCM model and establish its relationship with a modified GMM. The experimental results of the proposed approach are given in Section 4. Finally, some concluding remarks are provided.

2 FCMs algorithm

To deal with the problem of clustering N multivariate data points into K clusters, Dunn [23] introduced and later Bezdek [5] extended the FCMs clustering algorithm. In the standard FCM algorithm, the fuzzy objective function that needs to be minimised is given by

$$J_m = \sum_{i=1}^{N}\sum_{j=1}^{K} u_{ij}^m d(y_i,\ \mu_j) \tag{1}$$

where y_i, $i = (1, 2, \ldots, N)$, denotes the dataset in the $\boldsymbol{D}$-dimensional vector space, N is the total number of data points, K is the number of clusters, u_{ij} is the degree of membership of y_i in the jth cluster, m is the weighting exponent on each fuzzy membership function u_{ij}, μ_j is the prototype of the centre of cluster j and $d(y_i, \mu_j)$ is a distance measure between point y_i and cluster centre μ_j, called distance function. The Euclidean distance is usually used in standard FCM.

For image segmentation application, y_i represents the intensity value of the ith pixel, N is the total number of pixels in an image. $D = 1$ for greyscale image and $D = 3$ for RGB colour image. K is the number of regions of the segmented image (class), and $d(y_i, \mu_j)$ is a distance measure between image pixel intensity y_i and class centre μ_j. In fact, applying FCM for image segmentation is similar as applying FCM on data point clustering. The difference between them is that image pixels contain more spatial information among them according to different images content. Thus, it needs to consider more local spatial information for image segmentation application. In this paper, we adopt mean template as the spatial constraint.

Ichihashi *et al.* [24] introduced another FCM variant, using a regularisation to modify standard fuzzy objective function by KL information with constraint term $\sum_j \pi_j = 1$ and $\sum_i u_{ij} = 1$. Under this consideration, the modified fuzzy objective function becomes

$$J_\lambda = \sum_{i=1}^{N}\sum_{j=1}^{K} u_{ij} d(y_i,\ \mu_j) + \lambda \sum_{i=1}^{N}\sum_{j=1}^{K} u_{ij} \log\left(\frac{u_{ij}}{\pi_j}\right) \tag{2}$$

where λ is the model's degree of fuzziness of the fuzzy membership values and π_j is the prior probability of the jth cluster.

More recently, Ahmed *et al.* [4] proposed another modification of the FCM for image segmentation. The algorithm is formulated by modifying the objective function of the standard FCM to compensate for such inhomogeneities and to allow the labelling of a pixel to be influenced by the labels in its immediate neighbourhood. The modified fuzzy objective function is defined as follows

$$J_m = \sum_{i=1}^{N}\sum_{j=1}^{K} u_{ij}^m \left(d(y_i,\ \mu_j) + \frac{a}{N_R} \sum_{m \in \mathcal{N}_i} d\left(y_m,\ \mu_j\right) \right) \tag{3}$$

where y_i is the intensity value of the ith pixel, N is the total number of pixels in an image, y_m represents the neighbour of y_i, N_i is the neighbourhood of the ith pixel including the ith pixel itself and N_R represents its cardinality. The parameter a is used to control the effect of the neighbour's term.

doi: 10.1049/iet-ipr.2013.0178

3 Proposed method

3.1 Model establishment

It is noted that (3) is equivalent to the usage of mean template for distance function d. In this paper, we also apply mean template on prior probability π_j to incorporate local spatial information and component information. To demonstrate our algorithm, we first combine (2) and (3), with some modification for consideration of spatial constraints, to generate a new objective function

$$J = \frac{1}{2}\sum_{i=1}^{N}\sum_{j=1}^{K} u_{ij}\left(d(y_i,\ \mu_j) + \sum_{m\in\mathcal{N}_i}\frac{w_m}{R_i}d(y_m,\ \mu_j)\right) + \sum_{i=1}^{N}\sum_{j=1}^{K} u_{ij}\log\left(\frac{u_{ij}}{\pi_{ij}}\right) \tag{4}$$

where the distance function d in (4) is different from that in (2) and (3), which is defined by the multivariate Gaussian distribution p as follows

$$d(y_i,\ \mu_j) = -\log p(y_i|\theta_j) \tag{5a}$$

Here, θ_j represents the mean μ_j and covariance $\mathbf{\Sigma}_j$ of multivariate Gaussian distribution. The multivariate Gaussian distribution is given as follows

$$p(y_i|\theta_j) = \frac{1}{(2\pi)^{D/2}\left|\sum_j\right|^{1/2}}\exp\left\{-\frac{1}{2}(y_i-\mu_j)^{\mathrm{T}}\Sigma_j^{-1}(y_i-\mu_j)\right\} \tag{5b}$$

Then, we have

$$d(y_i,\ \mu_j) = \frac{1}{2}(y_i-\mu_j)^{\mathrm{T}}\Sigma_j^{-1}(y_i-\mu_j) + \frac{D}{2}\log 2\pi + \frac{1}{2}\log\mathbf{\Sigma}_j \tag{6}$$

In (4), N_i is the neighbourhood of the ith pixel, including the ith pixel. w_m is the weighting to control the influence of the neighbourhood pixels depending on their distance from the central pixel. R_i is the normalised factor, defined as

$$R_i = \sum_{m\in\mathcal{N}_i} w_m \tag{7}$$

A simple choice of the weighted parameter w_m in (4) is that $w_m = 1$ for all mth pixels and R_i equals the number of pixels in the neighbourhood window. However, to incorporate the spatial information and pixel intensity value information, the strength of w_m should decrease as the distance between pixel m and i increases. For this reason, we define w_m as the function of $L_{mi,}$ which is the spatial Euclidean distance between pixels m and i

$$w_m = \frac{1}{(2\pi\delta^2)^{1/2}}\exp\left(-\frac{L_{mi}^2}{2\delta^2}\right) \tag{8}$$

$$\delta = \frac{\text{neighbourhood window size} - 1}{4} \tag{9}$$

Comparing (4) with (2) and (3), it can be seen that there are no pre-defined parameters a or λ in our model. Note that the prior probability π_{ij} in (4) represents the prior distribution of pixel y_i belonging to class j, which satisfies the constraint

$$0 \le \pi_{ij} \le 1 \text{ and } \sum_{j=1}^{K}\pi_{ij} = 1 \tag{10}$$

Traditional estimation of fuzzy membership is in an FCM way. However, this derivation ignores the relationship between the neighbourhoods of image pixels, thus lacks of spatial information. One possible solution of this problem is the well-known HMRF model. However, the HMRF model is too complex and time consuming. In this paper, we introduce another algorithm to apply a mean template on posterior probability (membership). The mean template is utilised based on the relationship between our new FCM and GMM (see next subsection). Let us first recall the calculation of prior probability π_j in GMM

$$\pi_j = \frac{\sum_{i=1}^{N} z_{ij}}{\sum_{i=1}^{N}\sum_{j=1}^{K} z_{ij}} \tag{11}$$

where z_{ij} represents posterior probability of the pixel y_i belonging to the class x_i. The difference between prior probability π_j and posterior probability z_{ij} is that the y_i is observed in the latter case. In mathematical expression, prior probability $\pi_j = p(x_i = j)$ and posterior probability $z_{ij} = p(x_i = j|y_i)$. Following Ruspini [25], these probabilities can also be considered as fuzzy sets in the sense introduced by Zadeh [26], but also having a strong probabilistic interpretation. Inspired by (11), in our model, with consideration of spatial constraints, we have

$$\pi_{ij} = \frac{u_{ij}}{\sum_{j=1}^{K} u_{ij}} \tag{12}$$

We then apply a mean template on fuzzy membership function for calculating the prior probability, which yields

$$\pi_{ij} = \frac{\left(\sum_{m\in\mathcal{N}_i} w_m u_{mj}\right)^{\beta}}{\sum_{k=1}^{K}\left(\sum_{m\in\mathcal{N}_i} w_m u_{mk}\right)^{\beta}} \tag{13}$$

where N_i is the neighbourhood of the ith pixel. β is the strength factor and can be set as 2, 3, 4 … for increasing the performance. Here, we set $\beta = 2$. One possible choice of weighted parameter is $w_m = 1/\left(1 + L_{mi}^2\right)$. It is noted that (4) and (13) are equal to the standard GMM when we set the neighbourhood window size as 1×1 (note the difference between π_j in GMM and π_{ij} in our model). Thus, GMM can be considered as a special case of our model.

The major special characteristics of our algorithm are summarised below:

1. Our algorithm is free of parameter selection.
2. Our algorithm decreases the influence of the neighbourhood pixels with the increasing of their distance from the central pixel.
3. Our algorithm uses multivariate Gaussian distribution instead of traditional Euclidean distance (L_2 norm) in standard FCM algorithm.

4. Our algorithm uses mean template instead of HMRF to incorporate more local spatial information.

The graphic model of the proposed algorithm is shown in Fig. 1.

3.2 Parameter estimation

Let us first consider the derivation of the fuzzy membership function values. This can be obtained by minimising the objective function J over u under the constraints $\sum_{j=1}^{K} u_{ij} = 1$. Using the Lagrange multiplier, we have

$$J_u = J + \lambda\left(1 - \sum_{j=1}^{K} u_{ij}\right) \tag{14}$$

Taking the derivative of J_u with respect to u_{ij} and setting the result to zero, we have

$$u_{ij}^{(k+1)} = \frac{\pi_{ij}^{(k)} \exp\left\{-\frac{1}{2}\left(d_{ij}^{(k)} + \sum_{m\in\mathcal{N}_i} \frac{w_m}{R_i} d_{mj}^{(k)}\right)\right\}}{\sum_{h=1}^{K} \pi_{ih}^{(k)} \exp\left\{-\frac{1}{2}\left(d_{ih}^{(k)} + \sum_{m\in\mathcal{N}_i} \frac{w_m}{R_i} d_{mh}^{(k)}\right)\right\}} \tag{15}$$

Let us then consider the derivation of the updates of means μ_j and the covariance matrices $\mathbf{\Sigma}_j$. Using (6), ignoring the non-relative items, the expression of the objective function (4) yields

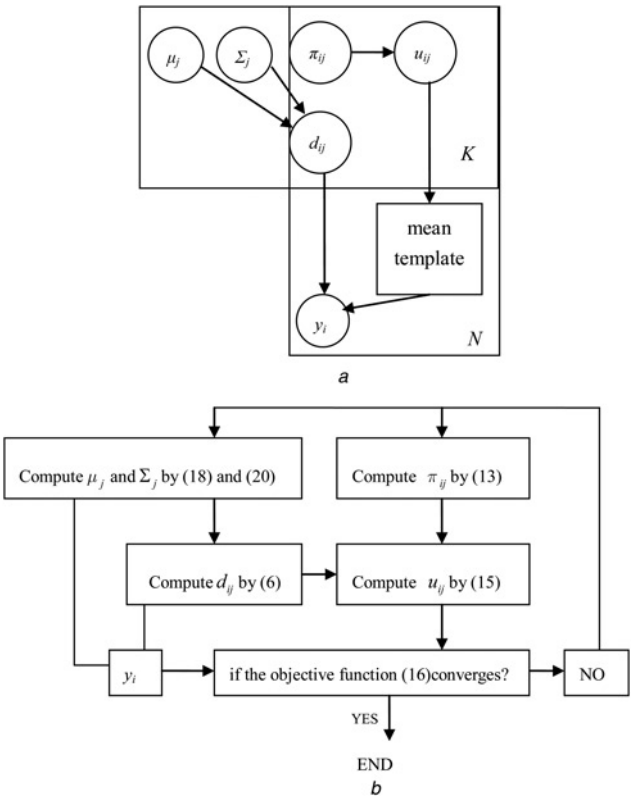

Fig. 1 *Graph model of the proposed algorithm*

a Graph representation
b Detail computation steps

$$J_{mc} = \frac{1}{2}\sum_{i=1}^{N}\sum_{j=1}^{K} u_{ij}\left(\frac{1}{2}(y_i-\mu_j)^{\mathrm{T}}\Sigma_j^{-1}(y_i-\mu_j) + \frac{1}{2}\log\mathbf{\Sigma}_j + \sum_{m\in\mathcal{N}_i}\left(\frac{1}{2}(y_m-\mu_j)^{\mathrm{T}}\Sigma_j^{-1}(y_m-\mu_j) + \frac{1}{2}\log\mathbf{\Sigma}_j\right)\right) \tag{16}$$

To obtain the estimates of mean, we need to minimise the objective function by solving $\partial J_{mc}/\partial\mu_j = 0$

$$\frac{\partial J_{mc}}{\partial \mu_j} = \sum_{i=1}^{N} u_{ij}\left(\Sigma_j^{-1}(y_i-\mu_j) + \sum_{m\in\mathcal{N}_i}\frac{w_m}{R_i}\Sigma_j^{-1}(y_m-\mu_j)\right) = 0 \tag{17}$$

The solution of (17) eventually yields

$$\mu_j^{(k+1)} = \frac{\sum_{i=1}^{N} u_{ij}^{(k)}\left\{y_{ij} + \sum_{m\in\mathcal{N}_i}\frac{w_m}{R_i}y_m\right\}}{2\sum_{i=1}^{N} u_{ij}^{(k)}} \tag{18}$$

To obtain the estimates of covariance matrices, we need to minimise the objective function by solving $\partial J_{mc}/\partial\Sigma_j^{-1} = 0$

$$\frac{\partial J_{mc}}{\partial \Sigma_j^{-1}} = \sum_{i=1}^{N} u_{ij}\left\{(y_i-\mu_j)(y_i-\mu_j)^{\mathrm{T}} - \mathbf{\Sigma}_j + \sum_{m\in\mathcal{N}_i}\frac{w_m}{R_i}\left((y_m-\mu_j)(y_m-\mu_j)^{\mathrm{T}} - \mathbf{\Sigma}_j\right)\right\} = 0 \tag{19}$$

The solution of (19) eventually obtains

$$\Sigma_j^{(k+1)} = \frac{\sum_{i=1}^{N} u_{ij}^{(k)}}{2\sum_{i=1}^{N} u_{ij}^{(k)}}\left\{\left(y_i-\mu_j^{(k)}\right)\left(y_i-\mu_j^{(k)}\right)^{\mathrm{T}} + \sum_{m\in\mathcal{N}_i}\frac{w_m}{R_i}\left(y_m-\mu_j^{(k)}\right)\left(y_m-\mu_j^{(k)}\right)^{\mathrm{T}}\right\} \tag{20}$$

For a deep understanding of our algorithm, we summarise the computation process of our algorithm as follows

Algorithm: parameter learning in our model

Step 1: use mean template for calculating the prior probability $\pi_{ij}^{(k)}$ given by (13).

Step 2: compute the fuzzy membership function $u_{ij}^{(k+1)}$ using (15).

Step 3: compute the quantities $\mu_j^{(k+1)}$ and $\Sigma_j^{(k+1)}$ by (18) and (20), respectively.

Step 4: terminate the iterations if the objective function converges; otherwise, increase the iteration ($k = k+1$) and repeat steps 1–4.

3.3 Connection to GMM

Let y_i, with dimension D, $i = (1, 2, \ldots, N)$, denote the intensity value at the ith pixel of an image and j ($j = 1, 2, \ldots, K$) denote

doi: 10.1049/iet-ipr.2013.0178

the corresponding class label of the ith pixel. GMM is defined as

$$p(y_i|\pi,\ \theta) = \sum_{j=1}^{K} \pi_j p(y_i|\theta_j) \tag{21}$$

where the probability π_j is the prior distribution of the pixel y_i belonging to the class x_i, and satisfies the constraints $0 \le \pi_j \le 1$ and $\sum_{j=1}^{K} \pi_j = 1$. y_i follows a conditional probability distribution $p(y_i|\theta_j)$ which is selected as Gaussian function and is defined in (5b).

Considering the spatial information on the prior probability, we introduce a new modified GMM as

$$p(y_i|\pi,\ \theta) = \sum_{j=1}^{K} \pi_{ij} \left[p(y_i|\theta_j) \prod_{m\in\mathcal{N}_i} p(y_m|\theta_j)^{\frac{w_m}{R_i}} \right]^{1/2} \tag{22}$$

The definition of parameters in (22) is the same as that in (7)–(9). It is noted that the exponent factor 1/2 is used for normalising probability distributions. In GMM, the integral of conditional probability should be equal to one. Compared (22) with (7), it is worth to point out that the usage of (arithmetic) mean template in FCM is equivalent to the usage of (geometric) mean template in GMM. We then apply the EM algorithm for parameter learning in our model. First, according to [2], the complete-data log likelihood function is calculated as

$$Q = \sum_i \sum_j z_{ij} \left[\log \pi_{ij} + \frac{1}{2} \log p(y_i|\theta_j) + \frac{1}{2} \sum_{m\in\mathcal{N}_i} \frac{w_m}{R_i} \log p(y_m|\theta_j) \right] \tag{23}$$

In E-step, the posterior probability can be calculated as

$$z_{ij}^{(k+1)} = \frac{\pi_{ij}^{(k)} \left[p\left(y_i|\theta_j^{(k)}\right) \prod_{m\in\mathcal{N}_i} p\left(y_m|\theta_j^{(k)}\right)^{\frac{w_m}{R_i}} \right]^{1/2}}{\sum_{h=1}^{K} \pi_{ih}^{(k)} \left[p\left(y_i|\theta_h^{(k)}\right) \prod_{m\in\mathcal{N}_i} p\left(y_m|\theta_h^{(k)}\right)^{\frac{w_m}{R_i}} \right]^{1/2}} \tag{24}$$

The M-step evaluates the mean and covariance as follows

$$\mu_j^{(k+1)} = \frac{\sum_{i=1}^{N} z_{ij}^{(k)} \left\{ y_{ij} + \sum_{m\in\mathcal{N}_i} \frac{w_m}{R_i} y_m \right\}}{2 \sum_{i=1}^{N} z_{ij}^{(k)}} \tag{25}$$

$$\Sigma_j^{(k+1)} = \frac{\sum_{i=1}^{N} z_{ij}^{(k)}}{2 \sum_{i=1}^{N} N} \left\{ \left(y_i - \mu_j^{(k)}\right)\left(y_i - \mu_j^{(k)}\right)^{\mathrm{T}} + \sum_{m\in\mathcal{N}_i} \frac{w_m}{R_i} \left(y_m - \mu_j^{(k)}\right)\left(y_m - \mu_j^{(k)}\right)^{\mathrm{T}} \right\} \tag{26}$$

In this section, we reveal the relationship between our fuzzy algorithm and GMM model. After some manipulation, it can be seen that (15), (18) and (20) are equal to (24)–(26), although they are derived from the FCMs algorithm and EM algorithm in modified GMM, respectively. Thus, our FCMs model can also be seen as a modified GMM model. Moreover, our model degrades to the standard GMM when we set the neighbourhood window size as 1×1 in (22).

4 Experimental results and discussion

In this section, we experimentally evaluate our algorithm in a set of synthetic images and real images. We also evaluate PFCM [9], extension of Gaussian mixture model (EGMM) [17], FCM_S1 and FCM_S2 [6], fuzzy local information c-means (FLICM) [3] and HMRF-FCM [19] for comparison. The compared methods are based on different types of models, and were published in different journals recently; thus, it is more significant to compare our algorithm with these state-of-the-art technologies. The source codes for the FLICM and HMRF-FCM algorithms can be downloaded from the authors' websites [27, 28]. Our experiments have been developed in MATLAB R2009b, and are executed on an Intel Pentium Dual-Core 2.2 GHZ central processing unit (CPU), 2G random access memory.

4.1 Synthetic images

In the first experiment, a three-class synthetic image (246 × 246, shown in Fig. 2*a*) is used to compare the performance of the proposed method with others. Fig. 2*b* shows the same image corrupted by Gaussian noise with zero mean and 0.15 variance. To evaluate the segmentation results, we employ the misclassification ratio (MCR) [21] in our experiments.

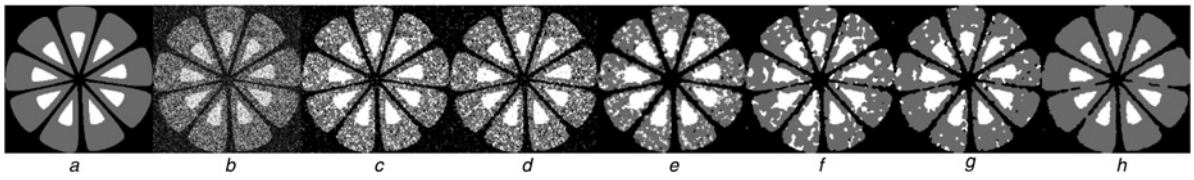

Fig. 2 *Synthetic images*

a Original three-class image
b Corrupted by Gaussian noise (zero mean and 0.15 variance)
c FCM_S1, MCR = 17.50% and t = 2.97 s
d FCM_S2, MCR = 18.22% and t = 3.61 s
e FLICM, MCR = 15.46% and t = 21.9 s
f HMRF-FCM, MCR = 12.10% and t = 230.74 s
g EGMM, MCR = 8.87% and t = 49.2 s
h Proposed method, MCR = 2.92% and t = 3.43 s

Table 1 MCR % and computation time of synthetic image with additive Gaussian noise for different methods

Methods	var = 0.06	var = 0.09	var = 0.12	var = 0.15	Computation time (s)
FCM_S1	4.18	7.69	13.18	17.50	2.97
FCM_S2	3.51	8.39	13.38	18.22	3.61
FLICM	3.02	7.24	10.13	15.46	21.9
HMRF-FCM	2.96	4.69	10.44	12.10	230.74
EGMM	1.63	2.86	4.90	8.87	49.2
proposed	1.46	1.98	2.41	2.92	3.43

The value of MCR is in the [0–100%] range, where lower values indicate better segmentation performance. The segmentation results of the noised image (Fig. 2*b*) by FCM_S1, FCM_S2, FLICM, HMRF-FCM, EGMM and the proposed method are shown in Figs. 2*c–h*. The class number is set to 3 based on previous experience. As we observe, FCM_S1 and FCM_S2 do not segment images well. Although FLICM, HMRF-FCM and EGMM can reduce the effect of noise to some extent, as [3, 17, 19] claim, they are still sensitive to heavy noise and misclassify some portions of pixels, as shown in Figs. 2*e–g*. However,

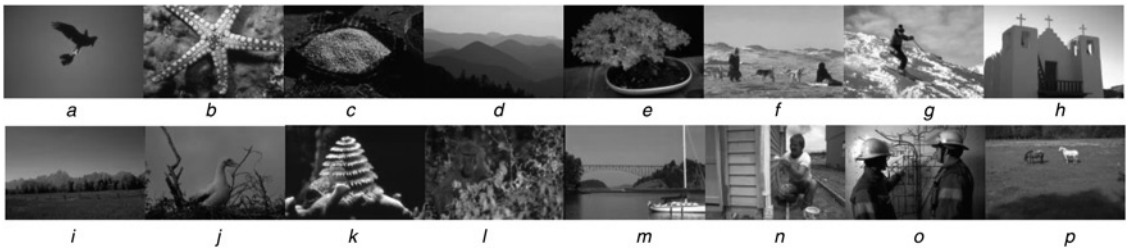

Fig. 3 *Original image from the Berkeley image segmentation dataset*

a 135 069
b 12 003
c 58 060
d 55 067
e 353 013
f 310 007
g 61 060
h 24 063
i 2092
j 8049
k 12 074
l 16 052
m 22 090
n 23 080
o 23 084
p 28 075

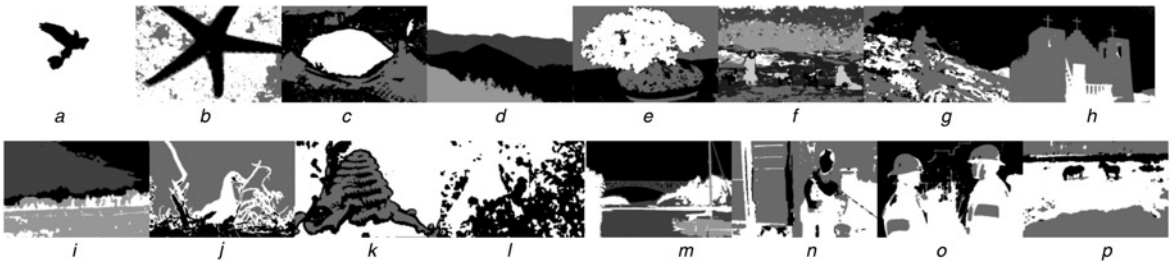

Fig. 4 *Image segmentation results by the proposed algorithm*

a 135 069
b 12 003
c 58 060
d 55 067
e 353 013
f 310 007
g 61 060
h 24 063
i 2092
j 8049
k 12 074
l 16 052
m 22 090
n 23 080
o 23 084
p 28 075

doi: 10.1049/iet-ipr.2013.0178

Table 2 Comparison of different methods for Berkeley image dataset, PR index, the highlighted values indicate the most optimal/best values

Image#	Class	PFCM	FCM_S1	FCM_S2	FLICM	HMRF-FCM	EGMM	Proposed
2092	4	0.806	0.743	0.743	**0.812**	0.743	0.779	0.781
8049	3	0.677	0.691	0.684	0.654	0.690	0.738	**0.740**
12 003	3	0.622	0.608	0.605	0.614	0.618	0.623	**0.732**
12 074	3	0.623	0.627	0.624	0.582	0.629	0.673	**0.677**
15 004	6	0.756	**0.758**	0.755	0.694	**0.758**	0.719	0.731
16 052	2	0.526	0.526	0.527	0.552	0.535	0.560	**0.567**
20 008	5	0.794	0.805	0.800	0.716	0.795	0.817	**0.825**
22 013	4	0.692	0.699	0.695	**0.724**	0.697	0.703	0.701
22 090	4	0.769	0.770	0.770	0.729	0.762	0.735	**0.803**
23 080	3	0.631	0.633	0.633	**0.658**	0.635	0.604	0.615
23 084	3	0.572	0.572	0.576	0.611	0.571	0.638	**0.644**
24 004	3	0.699	0.743	**0.748**	0.589	0.692	0.741	**0.748**
28 075	3	0.623	0.632	0.630	0.620	0.688	**0.690**	0.669
28 096	3	0.365	0.366	0.366	0.360	0.429	0.779	**0.804**
33 066	7	0.769	0.759	0.775	0.753	0.771	**0.829**	**0.829**
35 010	4	0.732	0.733	0.734	0.685	0.740	0.751	**0.762**
35 058	5	0.617	0.620	0.634	0.630	0.637	**0.676**	**0.676**
35 070	3	0.592	0.590	0.592	0.558	0.591	0.821	**0.824**
35 091	4	0.607	0.611	0.588	0.550	0.612	0.635	**0.636**
41 004	3	0.782	0.769	0.778	0.767	0.802	0.867	**0.876**
42 044	4	0.647	0.667	0.655	0.632	0.655	0.747	**0.750**
42 078	4	0.769	0.772	0.770	0.753	**0.780**	0.741	0.728
43 070	3	0.591	0.587	0.592	**0.712**	0.666	0.668	0.628
46 076	4	0.808	0.715	0.715	0.725	0.826	0.828	**0.845**
48 055	4	0.701	0.705	0.703	0.677	0.705	0.847	**0.869**
54 005	4	0.464	0.462	0.466	0.453	0.463	0.483	**0.485**
55 067	4	0.887	0.879	0.869	0.879	0.888	**0.891**	0.890
55 075	7	0.763	0.779	0.779	0.745	0.795	0.850	**0.871**
56 028	5	0.622	0.622	0.624	0.572	0.629	0.679	**0.688**
58 060	3	0.570	0.573	0.563	0.584	0.615	0.622	**0.645**
60 079	3	0.645	0.654	0.652	0.632	0.654	**0.954**	0.949
61 086	8	0.743	0.750	0.753	0.739	**0.780**	0.733	0.762
65 010	10	0.749	0.749	0.749	0.721	0.75	0.765	**0.77**
65 019	5	0.767	0.771	0.768	0.777	0.758	0.781	**0.789**
65 132	6	0.719	0.723	0.721	0.719	0.715	0.740	**0.742**
66 075	3	0.575	0.574	0.574	0.570	0.578	**0.705**	**0.705**
67 079	4	0.751	0.75	0.751	0.697	**0.758**	0.742	0.739
68 077	6	0.729	0.745	0.742	0.681	0.756	0.792	**0.800**
69 020	3	0.567	0.535	0.534	0.552	0.559	0.605	**0.676**
76 002	5	0.777	0.779	0.779	**0.801**	0.772	0.765	0.767
78 019	6	0.826	0.826	0.827	0.799	0.831	0.835	**0.838**
80 099	2	0.510	0.509	0.509	0.523	0.622	**0.876**	0.862
87 065	3	0.523	0.523	0.523	0.522	0.523	0.524	**0.525**
92 059	4	0.584	0.590	0.589	0.613	0.607	0.613	**0.622**
94 079	3	0.528	0.542	0.538	0.557	0.528	**0.697**	0.648
95 006	4	0.615	0.629	0.620	0.608	0.617	0.634	**0.653**
97 017	5	0.724	0.733	0.730	0.75	0.723	0.842	**0.850**
100 075	3	0.653	0.661	0.661	0.621	0.662	0.679	**0.691**
100 080	3	0.657	0.658	0.658	0.692	0.693	0.714	**0.718**
100 098	3	0.646	**0.654**	0.65	0.632	0.651	0.626	0.63
103 041	3	0.579	0.578	0.578	0.589	0.575	0.572	**0.593**
105 019	2	0.591	0.574	0.577	0.659	0.634	**0.947**	0.903
108 041	3	0.569	0.571	0.569	0.564	0.577	0.579	**0.592**
109 034	3	0.589	0.593	0.589	0.591	**0.597**	0.568	0.581
112 082	4	0.702	0.715	0.714	0.685	0.718	0.739	**0.742**
113 009	3	0.599	0.605	0.602	0.596	0.611	0.674	**0.684**
113 044	3	0.729	0.678	0.678	0.649	0.67	0.819	**0.832**
117 054	4	0.665	0.675	0.671	0.681	0.668	0.681	**0.685**
118 020	4	0.683	0.684	0.685	0.681	0.689	0.759	**0.764**
124 084	3	0.708	0.510	0.506	0.510	0.526	0.558	**0.781**
126 039	4	0.731	0.733	0.731	0.726	0.709	**0.743**	**0.743**
130 034	3	0.447	0.453	0.454	0.443	0.48	**0.484**	0.441
135 037	3	0.581	**0.582**	0.581	0.559	0.581	0.578	0.578
135 069	2	**0.985**	0.981	0.981	0.983	0.984	**0.985**	0.972
138 032	3	0.525	0.527	0.527	0.527	**0.533**	0.510	0.523
138 078	5	0.811	0.815	0.816	0.817	0.832	0.853	**0.869**
140 055	6	0.74	0.738	0.745	0.686	0.75	0.759	**0.764**
140 075	5	0.733	0.739	0.738	0.719	0.741	0.795	**0.817**
144 067	5	0.791	0.806	0.802	0.764	0.803	0.809	**0.827**
145 014	8	0.791	0.788	0.798	0.77	0.798	0.817	**0.824**
145 053	6	0.761	0.761	0.762	0.77	0.768	0.773	**0.774**
147 062	3	0.599	0.662	0.663	0.599	0.6	0.703	**0.724**
151 087	3	0.682	0.687	0.689	0.665	0.692	0.768	**0.864**

Continued

TABLE 2 *Continued*

Image#	Class	PFCM	FCM_S1	FCM_S2	FLICM	HMRF-FCM	EGMM	Proposed
153 077	5	0.689	0.691	0.689	0.699	0.692	0.729	**0.75**
155 060	3	0.733	0.742	0.742	**0.757**	0.744	0.626	0.639
156 079	3	0.702	0.706	0.706	0.533	0.713	**0.752**	0.748
157 036	4	0.689	0.689	0.693	0.699	0.7	0.732	**0.741**
159 045	3	0.609	0.615	0.613	0.617	0.609	0.629	**0.631**
159 091	4	0.574	0.579	0.579	0.589	0.581	0.612	**0.613**
161 062	3	0.773	0.775	0.775	0.537	0.829	**0.836**	0.833
163 014	4	0.685	0.708	0.707	0.684	0.695	0.744	**0.756**
163 062	3	0.748	0.758	0.755	0.731	0.761	0.841	**0.844**
166 081	5	0.736	0.748	0.744	0.713	0.74	0.799	**0.803**
169 012	3	0.6	0.607	0.6	0.602	0.597	0.629	**0.638**
239 007	3	0.665	0.633	0.634	0.645	0.668	0.671	**0.687**
61 060 + 0.01 noise	3	0.603	0.617	0.627	0.625	0.575	0.639	**0.698**
310 007 + 0.01 noise	7	0.619	0.664	0.661	0.708	0.677	0.733	**0.738**
353 013 + 0.01 noise	3	0.585	0.633	0.636	0.663	0.741	0.757	**0.783**
361 084 + 0.01 noise	6	0.782	0.808	0.805	0.783	0.706	0.841	**0.851**
365 025 + 0.01 noise	5	0.719	0.727	0.728	0.749	0.727	0.732	**0.757**
15 088 + 0.02 noise	2	0.699	0.656	0.654	0.717	0.855	0.851	**0.862**
24 063 + 0.02 noise	3	0.777	0.819	0.817	0.826	0.834	0.831	**0.839**
302 003 + 0.02 noise	3	0.696	0.705	0.705	0.713	0.715	0.708	**0.717**
374 067 + 0.02 noise	4	0.703	0.711	0.715	0.729	0.744	0.710	**0.782**
368 016 + 0.02 noise	4	0.656	0.703	0.697	**0.745**	0.702	0.684	0.712
368 078 + 0.03 noise	5	0.749	0.785	0.783	0.721	0.782	0.795	**0.804**
370 036 + 0.03 noise	6	0.643	0.687	0.677	0.525	0.721	**0.753**	0.725
372 047 + 0.03 noise	7	0.789	0.8	0.799	0.793	0.793	0.793	**0.804**
385 028 + 0.03 noise	7	0.759	0.778	0.776	0.7	0.775	0.78	**0.79**
388 016 + 0.03 noise	5	0.694	0.698	0.697	0.634	0.687	0.694	**0.699**
mean	–	**0.676**	**0.679**	**0.678**	**0.665**	**0.689**	**0.727**	**0.739**

we observe that the proposed method yields outstanding segmentation results compared with the poor performance of their competitors, as seen in Fig. 2*h*. The results obtained by different noise intensities are given in Table 1. As we observe, the proposed method obtains the best results compared with the other methods, and especially for heavy noised image segmentation.

The average computation CPU time t of different methods is shown in Fig. 2 and Table 1. It can be clearly seen that our algorithm is faster than other methods, except FCM_S1.

4.2 Real images

In this experiment, we evaluate the performance of the proposed method based on a subset of the Berkeley image dataset [29], which is comprised of a set of real-world colour images along with segmentation maps provided by different individuals. We use two types of indices to evaluate the quality of segmentation results. One is Rand index which evaluates the quality with respect to the reference result such as ground truth image. The other is Liu's F-measure which evaluates the colour difference in the CIELAB colour space [30] and also penalises the formation of large number of segments. The above two types of quality measures are used together to judge the efficiency and robustness of the proposed algorithm [31].

4.2.1 Probabilistic Rand (PR) index: We first employ the PR index [32] to evaluate the performance of the proposed method, with the multiple ground truths available for each image within the dataset. It has been shown that the PR index possesses the desirable property of being robust to segmentation maps that result from splitting or merging segments of the ground truth [33]. The PR index takes values between 0 and 1, with values closer to 0 (indicating an inferior segmentation result) and values closer to 1 (indicating a better result).

4.2.2 Liu's F-measure: The Liu's evaluation function F [34] is defined as

$$F(I) = \frac{1}{1000(N_1 \times N_2)} \sqrt{K} \sum_{j=1}^{K} \frac{e_j^2}{\sqrt{A_j}} \tag{27}$$

where I is the segmented image and $N_1 \times N_2$ is the image size, K is the number of regions of the segmented image, A_j is the number of pixels of the jth region and e_j is the colour error of region j. e_j is defined as the sum of the Euclidean distance of the colour vectors between the original image and the segmented image of each pixel in the region. The smaller value of $F(I)$ demonstrates the better segmentation result. We choose Liu's F-measure as one of our evaluation criteria since it gives an accurate measure of the colour differencing achieved by the segmentation algorithm and at the same time penalises large number of regions formed [31].

Fig. 3 shows some examples of original Berkeley images used for this segmentation experiment. These images with and without Gaussian noise are segmented by the proposed method, illustrated in Fig. 4. For fair comparison, we also evaluate the performance of PFCM, FCM_S1, FCM_S2, FLICM, HMRF-FCM and EGMM in addition to our methods. The class number K is set the same as in [17, 19]. The corresponding evaluation values by PR index and Liu's F-measure for 100 test images are presented in Tables 2 and 3, respectively. Compared with other methods, the proposed algorithm yields the best segmentation results with the highest average PR value which show a good match with human ground truth segmentations, and lowest average Liu's F-measure which shows an efficient colour differentiation. From Tables 2 and 3, it can be seen that our algorithm obtains 75 best segmentation results (highest PR index value) based on PR index value and 73 best segmentation results (lowest Liu's F value) based on Liu's F-measure in 100 Berkeley test images dataset.

doi: 10.1049/iet-ipr.2013.0178

Table 3 Comparison of different methods for Berkeley image dataset, Liu's *F*-measure (10^{-3}), the highlighted values indicate the most optimal/best values

Image#	Class	PFCM	FCM_S1	FCM_S2	FLICM	HMRF-FCM	EGMM	Proposed
2092	4	0.940	0.703	0.701	1.203	0.785	0.696	**0.692**
8049	3	1.308	1.278	1.293	1.352	1.356	**1.216**	**1.216**
12 003	3	7.627	7.395	7.458	9.165	7.312	5.891	**5.778**
12 074	3	1.829	1.798	1.816	2.515	1.763	**1.738**	1.789
15 004	6	5.537	7.605	5.414	7.578	5.267	5.548	**4.341**
16 052	2	1.031	1.007	1.011	1.031	0.983	0.832	**0.819**
20 008	5	1.796	1.637	1.750	4.912	1.656	1.757	**1.467**
22 013	4	3.007	2.923	2.962	2.934	2.946	2.922	**2.896**
22 090	4	0.729	0.733	0.734	0.881	0.876	0.792	**0.611**
23 080	3	1.133	1.127	1.127	1.207	1.129	0.674	**0.659**
23 084	3	11.00	11.05	11.03	11.74	10.34	**7.541**	7.642
24 004	3	1.731	1.151	1.105	3.146	1.814	1.074	**1.064**
28 075	3	1.063	1.030	1.038	1.361	1.079	0.979	**0.917**
28 096	3	0.846	0.857	0.857	0.869	0.860	**0.760**	0.772
33 066	7	1.171	1.188	1.205	1.480	1.157	0.889	**0.703**
35 010	4	2.903	2.825	2.764	4.759	2.512	1.881	**1.859**
35 058	5	3.765	3.747	3.812	5.709	3.739	3.439	**3.238**
35 070	3	2.928	2.895	2.878	3.770	**2.754**	2.855	2.792
35 091	4	2.535	2.438	3.507	4.368	2.506	1.766	**1.562**
41 004	3	0.795	0.822	0.797	0.762	0.699	0.382	**0.368**
42 044	4	0.551	0.576	0.570	0.597	0.591	**0.516**	0.531
42 078	4	1.144	1.154	1.146	1.144	1.161	0.906	**0.903**
43 070	3	0.925	0.915	0.919	1.048	0.961	0.672	**0.598**
46 076	4	3.342	3.352	3.338	3.866	3.277	3.234	**3.191**
48 055	4	3.664	3.189	3.264	5.888	3.758	2.459	**1.572**
54 005	4	**0.884**	0.915	0.916	0.931	0.933	0.962	0.896
55 067	4	0.278	0.278	0.277	0.297	**0.274**	0.276	0.276
55 075	7	4.189	3.895	3.953	5.469	3.794	4.059	**2.846**
56 028	5	2.112	2.076	2.061	2.062	1.989	**0.944**	0.997
58 060	3	6.290	5.818	5.945	5.601	5.828	4.618	**4.539**
60 079	3	0.224	0.222	0.222	0.244	0.219	**0.194**	0.200
61 086	8	2.586	2.409	2.418	2.967	2.188	1.619	**1.498**
65 010	10	4.927	4.516	4.578	11.65	4.459	3.7	**3.573**
65 019	5	15.91	14.84	15.43	20.02	14.89	12.32	**11.06**
65 132	6	2.347	2.318	2.308	2.431	2.354	2.043	**1.897**
66 075	3	4.938	4.877	4.945	5.302	5.032	**1.713**	1.771
67 079	4	0.964	0.941	0.912	3.691	0.568	**0.529**	0.682
68 077	6	1.989	1.973	1.963	3.909	1.842	1.510	**1.477**
69 020	3	1.836	1.791	1.791	2.172	1.780	0.830	**0.798**
76 002	5	2.822	2.706	2.725	3.385	2.589	**2.354**	2.362
78 019	6	2.36	1.935	2.227	2.341	2.197	1.520	**1.511**
80 099	2	0.619	0.620	0.620	0.612	0.612	**0.177**	0.205
87 065	3	1.17	1.18	1.17	1.196	1.143	1.07	**1.05**
92 059	4	1.87	1.87	1.87	1.982	1.862	1.782	**1.706**
94 079	3	0.685	0.648	0.659	0.669	0.649	**0.364**	0.394
95 006	4	5.368	4.546	4.741	5.455	4.363	3.425	**3.056**
97 017	5	2.217	2.163	2.163	2.13	2.129	1.848	**1.831**
100 075	3	1.759	1.679	1.689	2.136	1.729	1.345	**1.168**
100 080	3	1.569	1.543	1.548	2.527	2.5	**1.497**	1.532
100 098	3	1.023	1.016	1.021	**1.011**	1.019	1.069	1.079
103 041	3	0.993	0.971	0.958	0.920	0.948	0.739	**0.727**
105 019	2	0.155	0.145	0.146	0.139	**0.141**	0.151	0.149
108 041	3	0.788	0.776	0.779	0.774	0.777	0.713	**0.698**
109 034	3	1.173	1.138	1.137	1.153	1.134	**1.055**	1.074
112 082	4	0.979	0.933	0.933	2.245	0.855	0.574	**0.543**
113 009	3	2.355	2.263	2.309	2.557	2.188	1.405	**1.4**
113 044	3	3.148	4.084	4.297	4.352	4.778	1.416	**1.188**
117 054	4	0.189	0.181	0.182	0.179	0.181	0.181	**0.178**
118 020	4	4.549	4.695	4.624	4.999	4.359	2.404	**2.314**
124 084	3	12.00	11.69	12.00	31.14	11.59	10.27	**10.16**
126 039	4	1.068	**1.058**	1.063	1.212	1.169	1.063	1.075
130 034	3	0.858	0.805	0.813	0.88	0.833	0.617	**0.601**
135 037	3	0.508	0.509	0.508	0.621	0.51	**0.447**	**0.447**
135 069	2	0.061	0.060	0.061	0.157	**0.042**	0.050	0.056
138 032	3	0.145	0.143	0.144	0.144	0.142	0.138	**0.136**
138 078	5	0.95	0.873	0.921	0.921	0.872	0.518	**0.442**
140 055	6	8.972	5.185	8.946	17.19	8.845	5.146	**4.951**
140 075	5	14.97	14.49	15.08	18.01	14.11	8.554	**5.544**
144 067	5	3.618	3.293	3.366	4.083	3.316	2.976	**2.558**
145 014	8	3.474	2.596	2.818	6.474	2.914	2.118	**1.856**
145 053	6	3.258	3.231	3.272	3.603	3.414	**2.761**	3.347
147 062	3	5.073	6.319	6.214	5.162	5.037	4.112	**3.892**
151 087	3	2.153	2.139	2.136	2.224	2.108	1.894	**1.404**

Continued

TABLE 3 *Continued*

Image#	Class	PFCM	FCM_S1	FCM_S2	FLICM	HMRF-FCM	EGMM	Proposed
153 077	5	4.722	4.716	4.713	6.225	4.607	3.697	**2.123**
155 060	3	1.008	1.0	0.999	1.006	0.987	**0.889**	0.97
156 079	3	9.392	9.269	9.293	15.73	8.833	**6.026**	6.232
157 036	4	0.36	0.355	0.353	**0.348**	0.351	0.381	0.388
159 045	3	4.346	4.392	4.382	4.418	4.419	4.154	**4.105**
159 091	4	1.519	1.479	1.479	1.447	1.445	1.112	**1.07**
161 062	3	0.577	0.566	0.596	1.747	0.249	**0.231**	0.242
163 014	4	1.812	1.745	1.736	2.419	1.815	1.115	**0.988**
163 062	3	3.519	3.352	3.413	4.201	3.434	3.034	**2.999**
166 081	5	1.767	1.474	1.818	2.65	1.836	0.901	**0.897**
169 012	3	4.192	4.183	4.159	4.042	4.022	3.993	**3.948**
239 007	3	5.662	5.602	5.614	5.608	5.576	4.495	**4.44**
353 013 + 0.01 noise	3	7.228	6.410	6.438	8.265	6.280	5.764	**5.067**
310 007 + 0.01 noise	7	0.939	0.891	0.883	1.221	0.656	0.534	**0.457**
61 060 + 0.01 noise	3	0.473	0.437	0.475	0.348	0.377	0.381	**0.361**
361 084 + 0.01 noise	6	2.982	2.33	2.408	3.092	**1.048**	1.849	1.833
365 025 + 0.01 noise	5	2.744	2.636	2.628	2.576	2.579	2.559	**2.473**
15 088 + 0.02 noise	2	0.323	0.242	0.244	0.368	0.261	**0.235**	**0.235**
24 063 + 0.02 noise	3	**0.576**	0.577	**0.576**	0.585	0.578	0.578	0.584
374 067 + 0.02 noise	4	3.390	1.574	1.646	3.120	1.843	1.687	**1.304**
302 003 + 0.02 noise	3	2.021	1.980	1.979	1.973	1.948	1.948	**1.934**
368 016 + 0.02 noise	4	2.167	2.045	2.068	2.04	2.014	2.023	**1.851**
368 078 + 0.03 noise	5	7.631	4.530	4.669	12.07	4.308	4.166	**3.702**
370 036 + 0.03 noise	6	3.537	2.515	2.644	4.012	2.252	2.22	**2.162**
372 047 + 0.03 noise	7	4.559	3.613	3.544	4.478	3.613	3.026	**2.928**
385 028 + 0.03 noise	7	3.102	2.593	2.627	2.907	2.652	2.509	**1.87**
388 016 + 0.03 noise	5	1.06	1.033	1.039	1.509	1.043	**0.866**	1.021
mean	–	**2.873**	**2.693**	**2.758**	**3.81**	**2.675**	**2.128**	**1.973**
average computation time (s)	–	**21.62**	**16.24**	**16.11**	**28.61**	**159.59**	**63.77**	**18.85**

We also evaluate the average computation time of different methods for the considered 100 test images in Table 3. Although our algorithm is slower than FCM_S, it is still faster than its other competitors. The computation time of the proposed algorithm is nearly 2/3 of FLICM, 1/4 of EGMM and 1/8 of HMRF-FCM.

4.3 Colour image segmentation results

In this experiment, we try to segment the multidimensional RGB colour image into three classes: the blue sky, the red roof and the white wall. The original image (481 × 321) shown in Fig. 5*a* is corrupted by heavy Gaussian noise, with mean = 0 and covariance = 0.15. The noised image is shown in Fig. 5*b*, and the segmentation results of FCM_S1, FCM_S2, FLICM, HMRF-FCM, EGMM and our proposed method are shown in Figs. 5*c*–*h*, respectively. The accuracy of segmentation for FCM_S1 and FCM_S2 is quite poor. FLICM and HMRF-FCM obtain better results, but they are still sensitive to heavy noise. Although EGMM demonstrates better segmentation performance, it still misclassifies some portions of pixels at the edge region between the sky and the roof, as well as the edge region between the sky and the wall. The accuracy of the segmentation results from the proposed method, as shown in Fig. 5*h*, is better than that of other methods, obtaining the highest PR values.

We also evaluate the computation time for all methods in the previous experiment. The computation time t of the different methods is also presented in Fig. 5. It is noted that the computation of our methods is much faster than that of other methods, except for FCM_S methods. Compared with other methods, our models can be calculated more quickly and achieve the best segmentation results.

5 Conclusions

In this paper, the authors propose a new effective fuzzy clustering approach for image segmentation. Gaussian distance function and spatial constraints are incorporated into the fuzzy objective function by dealing with FCM in a Bayesian way. Thus, the authors model can be considered

Fig. 5 *RGB image segmentation with image noise*

a Original image
b Noised image
c FCM_S1, PR = 0.0.7587 and t = 4.23 s
d FCM_S2, PR = 0.7523 and t = 4.18 s
e FLICM, PR = 0.7794 and t = 28.18 s
f HMRF-FCM, PR = 0.8426 and t = 167.53 s
g EGMM, PR = 0.8461 and t = 66.61 s
h Proposed method, PR = 0.8545 and t = 16.97 s

doi: 10.1049/iet-ipr.2013.0178

as an extension of standard GMM and can degrade to GMM by setting the neighbourhood window size as 1×1. Moreover, they add weighting for distant pixels in order to distinguish among the contributions of different pixels, as the weighted parameters decrease with increasing distance. In their algorithm, the prior probability of an image pixel is influenced by the fuzzy membership (or posterior probability) of pixels in its immediate neighbourhood with the help of a mean template. Different from the HMRF model, their model is fully free of any empirically adjusted parameters and has less computation complexity. Compared with state-of-the-art technologies based on FCM, GMM, HMRF and their hybrid models, the experimental results demonstrate the improved robustness and effectiveness of their proposed algorithm.

6 Acknowledgments

This work was supported in part by the Canada Chair Research Program and the Natural Sciences and Engineering Research Council of Canada. This work was supported in part by the Science Research Foundation of Nanjing University of Information Science & Technology (20110431). This work was supported in part by the National Natural Science Foundation of China under grants 61105007 and 61103141. This work was supported in part by PAPD (a project funded by the Priority Academic Program Development of Jiangsu Higher Education Institutions).

7 References

1 McLachlan, G., Peel, D.: 'Finite mixture models' (John Wiley and Sons, New York, 2000)
2 Bishop, C.M.: 'Pattern recognition and machine learning' (Springer, 2006)
3 Krinidis, S., Chatzis, V.: 'A robust fuzzy local information C-means clustering algorithm', *IEEE Trans. Image Process.*, 2010, **5**, (19), pp. 1328–1337
4 Ahmed, M., Yamany, S., Mohamed, N., Farag, A., Moriarty, T.: 'A modified fuzzy c-means algorithm for bias field estimation and segmentation of MRI data', *IEEE Trans. Med. Imaging*, 2002, **21**, pp. 193–199
5 Bezdek, J.: 'Pattern recognition with fuzzy objective function algorithms' (Plenum, New York, 1981)
6 Chen, S., Zhang, D.: 'Robust image segmentation using FCM with spatial constraints based on new Kernel-induced distance measure', *IEEE Trans. Syst. Man Cybern.*, 2004, **34**, (4), pp. 1907–1916
7 Pham, D., Prince, J.L.: 'An adaptive fuzzy c-means algorithm for image segmentation in the presence of intensity inhomogeneities', *Pattern Recognit. Lett.*, 1999, **20**, pp. 57–68
8 Hathaway, R.J., Bezdek, J.C.: 'Generalized fuzzy c-means clustering strategies using L_p norm distances', *IEEE Trans. Fuzzy Syst.*, 2000, **8**, (5), pp. 576–582
9 Pal, N.R., Pal, K., Keller, J.M., Bezdek, J.: 'A possibilistic fuzzy c-means clustering algorithm', *IEEE Trans. Fuzzy Syst.*, 2005, **13**, (4), pp. 517–530
10 Yu, J., Yang, M.S.: 'A generalized fuzzy clustering regularization model with optimality tests and model complexity analysis', *IEEE Trans. Fuzzy Syst.*, 2007, **15**, (5), pp. 904–915
11 Nefti, S., Oussalah, M., Kaymak, U.: 'A new fuzzy set merging technique using inclusion-based fuzzy clustering', *IEEE Trans. Fuzzy Syst.*, 2008, **16**, (1), pp. 145–161
12 Tran, D., Wagner, M.: 'Fuzzy Gaussian mixture models for speaker recognition', *Spec. Issue Aust. J. Intell. Inf. Process. Syst. (AJIIPS)*, 1998, **5**, (4), pp. 293–300
13 Ramathilaga, S., Leu, J.J.Y., Huang, Y.M.: 'Adapted mean variable distance to fuzzy-C means for effective image clustering'. 2011 First Int. Conf. Robot, Vision and Signal Processing (RVSP), 2011, pp. 48–51
14 Tolias, Y.A., Panas, S.M.: 'Image segmentation by a fuzzy clustering algorithm using adaptive spatially constrained membership functions', *IEEE Trans. Syst. Man Cybern. A, Syst. Hum.*, 1998, **28**, (3), pp. 359–369
15 Liew, A.C., Yan, H., Law, N.F.: 'Image segmentation based on adaptive cluster prototype estimation', *IEEE Trans. Fuzzy Syst.*, 2005, **13**, (4), pp. 444–453
16 Chuang, K.S., Tzeng, H.L., Chen, S., Wu, J., Chen, T.-J.: 'Fuzzy c-means clustering with spatial information for image segmentation', *Comput. Med. Imaging Graph.*, 2006, **30**, (1), pp. 9–15
17 Thanh, M.N., Wu, Q.M.J., Ahuja, S.: 'An extension of the standard mixture model for image segmentation', *IEEE Trans. Neural Netw.*, 2010, **21**, (8), pp. 1326–1338
18 Thanh, M.N., Wu, Q.M.J.: 'Gaussian-mixture-model-based spatial neighborhood relationships for pixel labeling problem', *IEEE Trans. Syst. Man Cybern. B*, 2012, **42**, (1), pp. 193–202
19 Chatzis, S.P., Varvarigou, T.A.: 'A fuzzy clustering approach toward hidden markov random field models for enhanced spatially constrained image segmentation', *IEEE Trans. Fuzzy Syst.*, 2008, **16**, (5), pp. 1351–1361
20 Rabiner, L.R.: 'A tutorial on hidden Markov models and selected applications in speech recognition', *Proc. IEEE*, 1989, **77**, (2), pp. 257–286
21 Zhang, Y., Brady, M., Smith, S.: 'Segmentation of brain MR images through a hidden Markov random field model and the expectation maximization algorithm', *IEEE Trans. Med. Imaging*, 2001, **20**, (1), pp. 45–57
22 Besag, J.: 'Statistical analysis of non-lattice data', *Statistician*, 1975, **24**, pp. 179–195
23 Dunn, J.: 'A fuzzy relative of the ISODATA process and its use in detecting compact well separated clusters', *J. Cybern.*, 1974, **3**, pp. 32–57
24 Ichihashi, H., Miyagishi, K., Honda, K.: 'Fuzzy c-means clustering with regularization by K-L information'. Proc. 10th IEEE Int. Conf. Fuzzy Systems, 2001, pp. 924–927
25 Ruspini, E.: 'A new approach to clustering', *Inf. Control*, 1969, **15**, pp. 22–32
26 Zadeh, L.: 'Fuzzy sets', *Inf. Control*, 1965, **8**, pp. 338–353
27 Available at http://www.infoman.teikav.edu.gr/~stkrini/pages/develop/FLICM/FLICM.html
28 Available at http://www.web.mac.com/soteri0s/Sotirios_Chatzis/Software.html
29 Martin, D., Fowlkes, C., Tal, D., Malik, J.: 'A database of human segmented natural images and its application to evaluating segmentation algorithms and measuring ecological statistics'. Proc. Eighth IEEE Int. Conf. Computer Vision, Vancouver, BC, Canada, 2001, vol. 2, pp. 416–423
30 Wyszecki, G., Stiles, W.S.: 'Color science—concepts and methods, quantitative data and formulae' (Wiley Inter-Science Publications, New York, 2000)
31 Hanmandlu, M., Verma, O.P., Susan, S., Madasu, V.K.: 'Color segmentation by fuzzy co-clustering of chrominance color features', *Neurocomputing*, *In press*, 2013
32 Unnikrishnan, R., Pantofaru, C., Hebert, M.: 'A measure for objective evaluation of image segmentation algorithms', *IEEE Conf. Comput. Vis. Pattern Recognit.*, 2005, **3**, pp. 34–41
33 Unnikrishnan, R., Hebert, M.: 'Measures of similarity'. Proc. IEEE Workshop Computer Vision and Applications, 2005, pp. 394–400
34 Liu, J., Yang, Y.H.: 'Multiresolution color image segmentation', *IEEE Trans. Pattern Anal. Mach. Intell.*, 2005, **16**, (7), pp. 530–549